JOURNAL OF BACTERIOLOGY, Nov. 2003, p. 6686–6694 Vol. 185, No. 22
0021-9193/03/$08.00+0 DOI: 10.1128/JB.185.22.6686–6694.2003


# Synthesis and Deformylation of *Staphylococcus aureus* δ-Toxin Are Linked to Tricarboxylic Acid Cycle Activity

Greg A. Somerville,[1]* Alan Cockayne,[2] Manuela Dürr,[3] Andreas Peschel,[3] Michael Otto,[1] and James M. Musser[1]

*Laboratory of Human Bacterial Pathogenesis, Rocky Mountain Laboratories, National Institute of Allergy and Infectious Diseases, National Institutes of Health, Hamilton, Montana 59840[1]; Institute of Infections and Immunity, University of Nottingham, Nottingham NG7 2UH, United Kingdom[2]; and Microbial Genetics, University of Tübingen, 72076 Tübingen, Germany[3]*

Received 10 July 2003/Accepted 21 August 2003

**In bacteria, translation initiates with formyl-methionine; however, the N-terminal formyl group is usually removed by peptide deformylase, an enzymatic activity requiring iron. *Staphylococcus aureus* δ-toxin is a 26-amino-acid polypeptide secreted predominantly with a formylated N-terminal methionine, which led us to investigate regulation of δ-toxin deformylation. We observed that during exponential and early postexponential growth, δ-toxin accumulated in the culture medium in formylated and deformylated forms. In contrast, only formylated δ-toxin accumulated after the early postexponential phase. The transition from producing both species of δ-toxin to producing only formyl-methionine-containing δ-toxin coincided with increased tricarboxylic acid (TCA) cycle activity. The TCA cycle contains several iron-requiring enzymes, which led us to hypothesize that TCA cycle induction depletes the iron in the culture medium, thereby inhibiting peptide deformylase activity. As expected, *S. aureus* depletes the iron in the culture medium between the postexponential and stationary phases of growth. Inhibition of δ-toxin deformylation was relieved by TCA cycle inactivation or by addition of supplemental iron to the culture medium. Of interest, peptides containing formyl-methionine are potent chemoattractants for neutrophils, suggesting that δ-toxin deformylation may have functional consequences. We found neutrophil chemotactic activity only with formylated δ-toxin. The *S. aureus* TCA cycle is derepressed upon depletion of rapidly catabolizable carbon sources; this coincides with the transition to producing only formylated δ-toxin and results in an increased inflammatory response. The proinflammatory response should increase host cell damage and result in the release of nutrients. Taken together, these results establish that there is an important linkage between bacterial metabolism and pathogenesis.**

*Staphylococcus aureus* uses a complex regulatory network to control the expression of virulence factors. Central to this regulatory network is the accessory gene regulatory (*agr*) locus (15, 19). This locus consists of two divergently transcribed RNAs, encoding a density-dependent autoinducing system and an RNA effector molecule (RNAIII) (16). RNAIII acts primarily at the level of transcription but also has been shown to posttranscriptionally regulate alpha-toxin (*hla*) production; however, the exact mechanism of regulation is not known (17). In addition to its regulatory role, RNAIII is the mRNA for δ-toxin (*hld*) (11). The mature form of δ-toxin is a heat-stabile, 26-amino-acid peptide that inserts into and disrupts membranes (4). Additionally, it has been implicated in the prevention of biofilm formation and in stimulation of the oxidative burst of human neutrophils (22, 28). However, the precise function of δ-toxin in *S. aureus* pathogenesis has yet to be elucidated.

Recently, workers in our laboratory reported construction and characterization of an *S. aureus* aconitase (*acnA*) mutant (24). During the course of that study, it was observed that significantly more RNAIII was present in the aconitase mutant than in the wild-type strain in the stationary phase. These data led us to hypothesize that the aconitase mutant strain should produce significantly more δ-toxin than the isogenic wild-type strain produces. To test this hypothesis, the concentration of δ-toxin was determined by high-performance liquid chromatography (HPLC) throughout the growth cycle. Analysis of the HPLC chromatographs revealed the presence of two species of δ-toxin in the culture supernatants corresponding to the formylated and deformylated forms of δ-toxin. Interestingly, in wild-type strain SA564 the deformylation of δ-toxin was temporally controlled and coincided with induction of the tricarboxylic acid (TCA) cycle. TCA cycle inactivation eliminated temporal control of δ-toxin deformylation, demonstrating that there is linkage between the TCA cycle and δ-toxin deformylation. In this report, we describe an investigation of this linkage.

## MATERIALS AND METHODS

**Bacterial strains and growth conditions.** *S. aureus* strain SA564 and an isogenic mutant strain with aconitase inactivated (SA564-*acnA*::*ermB*) have been described previously (24). *S. aureus* strains were grown in tryptic soy broth (TSB) (BD Biosciences) or on TSB containing 15 g of agar per liter. Liquid cultures were grown in TSB at 37°C with a flask volume-to-medium volume ratio of 10:1 and were aerated by shaking at 225 rpm.

**Determination of δ-toxin concentration.** Aliquots of bacteria (1.5 ml) were centrifuged for 5 min at 20,800 × *g* in a refrigerated centrifuge, and supernatants were removed and stored at −20°C until they were used. The concentration of δ-toxin was measured by HPLC as described previously (18). The method used for purification of δ-toxin for the chemotaxis assays has been described previously (18), except that the column size was increased and 50 ml of culture supernatant was used. Formylated δ-toxin and deformylated δ-toxin were identified by using an Agilent 1100 series chromatographic system equipped with a

* Corresponding author. Mailing address: Laboratory of Human Bacterial Pathogenesis, Rocky Mountain Laboratories, National Institute of Allergy and Infectious Diseases, National Institutes of Health, 903 South 4th Street, Hamilton, MT 59840. Phone: (406) 363-9313. Fax (406) 363-9493. E-mail: gsomerville@niaid.nih.gov.

diode array detector and an LCMSD Trap VL mass spectrometer with an electrospray source (Agilent Technologies). The mass spectrometer was set to the positive mode with a target mass of 1,000 and a trap target of 50,000. The masses of formylated δ-toxin and deformylated δ-toxin were determined by averaging the mass spectra taken during elution of the corresponding peaks and by using the Agilent LCMSD Trap data analysis software for charge deconvolution.

**Enzymatic activity assays.** Cell-free lysates of *S. aureus* were prepared as follows. Aliquots (3 ml) were harvested at different times and suspended in 1.5 ml of lysis buffer containing 90 mM Tris (pH 8.0), 100 μM fluorocitrate, and 50 μg of lysostaphin (AMBI) per ml. The samples were incubated at 37°C for 10 min and passed through a French press twice at 15,000 lb/in$^2$. The lysates were centrifuged for 5 min at 20,800 × *g* at 4°C. The aconitase activities in the resulting cell-free lysate were assayed as described previously (24). For citrate synthase assays, bacteria were harvested and treated as described above, except that the cells were suspended in CS lysis buffer containing 20 mM Tris (pH 8.0), 1 mM EDTA, 20% glycerol, and 50 μg of lysostaphin per ml. The cell-free lysate was assayed for citrate synthase activity by using the method described by Weitzman (29). One unit of citrate synthase activity was defined as the quantity of enzyme that catalyzed the formation of 1 μmol of coenzyme A-SH min$^{-1}$ from oxaloacetate and acetyl-coenzyme A. For isocitrate dehydrogenase assays, bacteria were harvested and treated as described above, except that the cells were suspended in a solution containing 20 mM Tris (pH 7.5), 1 mM trisodium citrate, 5 mM $MnCl_2$, 10% glycerol, and 50 μg of lysostaphin per ml. Enzymatic activity was determined by the method of Williamson and Corkey (30). One unit of isocitrate dehydrogenase activity was defined as the amount of enzyme that produced an increase in $A_{340}$ of 0.01 U min$^{-1}$.

Peptide deformylase activity was assayed as described previously (13); however, the levels of peptide deformylase activity detectable in cell lysates were insufficient to allow a direct assay of enzyme activity during growth under standard conditions. The total protease activities present in culture supernatants were determined by using the universal protease substrate according to the manufacturer's specifications (Roche). Protein concentrations were determined by the method of Lowry et al. (14).

**Northern blot analysis.** Total RNA was isolated with a FastRNA Pro Blue kit (Qbiogene). Northern blot analysis of RNAIII and *pdf*1 transcripts was performed as described previously (20). The blot was probed with [$^{32}$P]dATP-labeled (RadPrime DNA labeling kit; GibcoBRL) PCR products amplified from SA564 genomic DNA. Prior to use the nucleotide sequences of the PCR products were verified by using fluorescent dye terminator chemistry for both strands. The integrated density values of bands on autoradiographs were determined with the TotalLab software (Nonlinear Dynamics Ltd.)

**Determination of iron contents of staphylococcal cells and culture supernatants.** SA564 or SA564-*acnA*::*ermB* was grown in TSB as described above and harvested by centrifugation at 10,000 × *g* for 10 min after 3, 6, or 12 h of incubation. Bacterial pellets were washed twice in Chelex-treated deionized water (3% [wt/vol] Chelex 100 [Sigma] overnight). The washed pellets were then dried at 80°C for 12 h and transferred to preweighed polypropylene tubes (Greiner), and dry weights were determined. The dried pellets were then hydrolyzed for 4 h at 80°C in 30% (vol/vol) nitric acid (Fisher). Each clear hydrolysate was centrifuged at 13,000 × *g* for 10 min, and the supernatant was retained for analysis. Culture supernatants were filter sterilized and hydrolyzed for 8 h at 80°C following addition of enough nitric acid so that it accounted for 30% of the final volume. All samples were analyzed with a Perkin-Elmer Optima 3300RL inductively coupled plasma-atomic emission spectrometer that was calibrated by using a 1-mg/liter multiple-element solution in a 1% nitric acid matrix.

**Neutrophil chemotaxis.** Venous blood from healthy human volunteers was collected in heparin-containing tubes (Vacuette; Greiner Bio-One), and neutrophils were isolated as described previously (26). Briefly, blood was diluted 1:1 (vol/vol) with phosphate-buffered saline and layered onto a gradient of Ficoll (Pharmacia) and Histopaque (density, 1.119 g/ml; Sigma). After centrifugation for 20 min at 320 × *g*, neutrophils were collected from the Histopaque phase. The cells were subjected to a brief hypotonic shock with distilled water to disrupt residual erythrocytes, washed, and suspended at a concentration of 5 × 10$^6$ cells/ml in Hanks' balanced salt solution containing 0.05% human serum albumin (Central Laboratory of Blood Transfusion Services, Amsterdam, The Netherlands).

Chemotaxis of neutrophils toward *N*-formyl-methionyl-leucyl-phenylalanine and δ-toxin was monitored with fluorescently labeled neutrophils and a 24-well microtiter plate Transwell system (Costar) containing a prewetted 3-μm-pore-size polycarbonate filter, as described previously (27). Briefly, a preparation containing 5 × 10$^6$ neutrophils/ml was labeled with 3.3 μM 2′,7′-bis-(2-carboxyethyl)-5-(and -6)-carboxyfluorescein acetoxymethyl ester (BCECF-AM) (Molecular Probes) for 20 min at room temperature and washed, and the neutrophils were then suspended at the same density in Hanks' balanced salt solution containing 0.05% human serum albumin. The upper Transwell compartment was filled with 100 μl of cells and placed into a well containing 600 μl of control buffer or chemoattractants. After incubation at 37°C in 5% $CO_2$ for 60 min, the inserts were removed, and the fluorescence was determined with a fluorescence reader (FL600; BIO TEK Instruments) with a 485-nm excitation filter and a 530-nm emission filter. Control wells containing only BCECF-AM-labeled cells were included to obtain a background fluorescence value. The percentage of neutrophils that migrated toward δ-toxin was calculated by subtracting the fluorescence of neutrophils that migrated spontaneously when no stimulus was added from the fluorescence of samples. The fluorescence of 100 μl of BCECF-AM-labeled neutrophils was defined as 100%.

## RESULTS

**δ-Toxin production.** We recently reported that *acnA* inactivation significantly increased the stationary-phase level of RNAIII compared to the level in the isogenic wild-type strain (24). The mRNA for δ-toxin is contained within RNAIII, which led us to hypothesize that a culture of the *acnA* mutant strain (SA564-*acnA*::*ermB*) should have a significantly higher concentration of δ-toxin in the culture supernatant. Determination of the concentrations of δ-toxin in the culture supernatants of strains SA564 and SA564-*acnA*::*ermB* (18) revealed that both the *acnA* mutant and the wild-type strain began accumulating δ-toxin late in the exponential phase of growth (Fig. 1A and B). However, the concentration of δ-toxin in the culture supernatant of wild-type strain SA564 was nearly fourfold greater than that in the culture supernatant of the isogenic *acnA* mutant strain after 12 h of growth. These data demonstrate that a functional aconitase is required for maximal δ-toxin production and suggest at least four possibilities to explain the decreased δ-toxin production. First, it is possible that TCA cycle inactivation decreases the growth yield and thus there are fewer bacteria producing δ-toxin. A second possibility is that aconitase inactivation limits the ability of the bacteria to synthesize glutamate. A third possibility is that the *acnA* mutant strain produces greater levels of protease activity; hence, δ-toxin is more rapidly degraded. Finally, it is possible that TCA cycle inactivation prevents the postexponential-growth-phase catabolism of acetate (24), resulting in a culture medium pH that is lower than that of the wild-type strain and potentially decreasing δ-toxin production.

Based on the observation that TCA cycle inactivation decreased the growth yield of the aconitase mutant strain compared to the growth yield of the wild-type strain (24), it is reasonable to speculate that a decreased growth yield should result in decreased δ-toxin production. The growth yields of both the wild-type and *acnA* mutant strains could be increased by addition of certain amino acids to the culture medium (Fig. 2). Supplementation of the culture medium with 25 mM serine increased the growth yield, but the total concentration of δ-toxin produced by the aconitase mutant was equivalent to the concentration produced in the unsupplemented culture medium (Fig. 2). These results demonstrate that the decreased production of δ-toxin by the aconitase mutant strain compared to the production by the wild-type strain is independent of the growth yield.

Glutamate auxotrophy can be caused by an inability to generate α-ketoglutarate, a TCA cycle intermediate that provides the carbon skeleton for glutamate. Hence, the decrease in

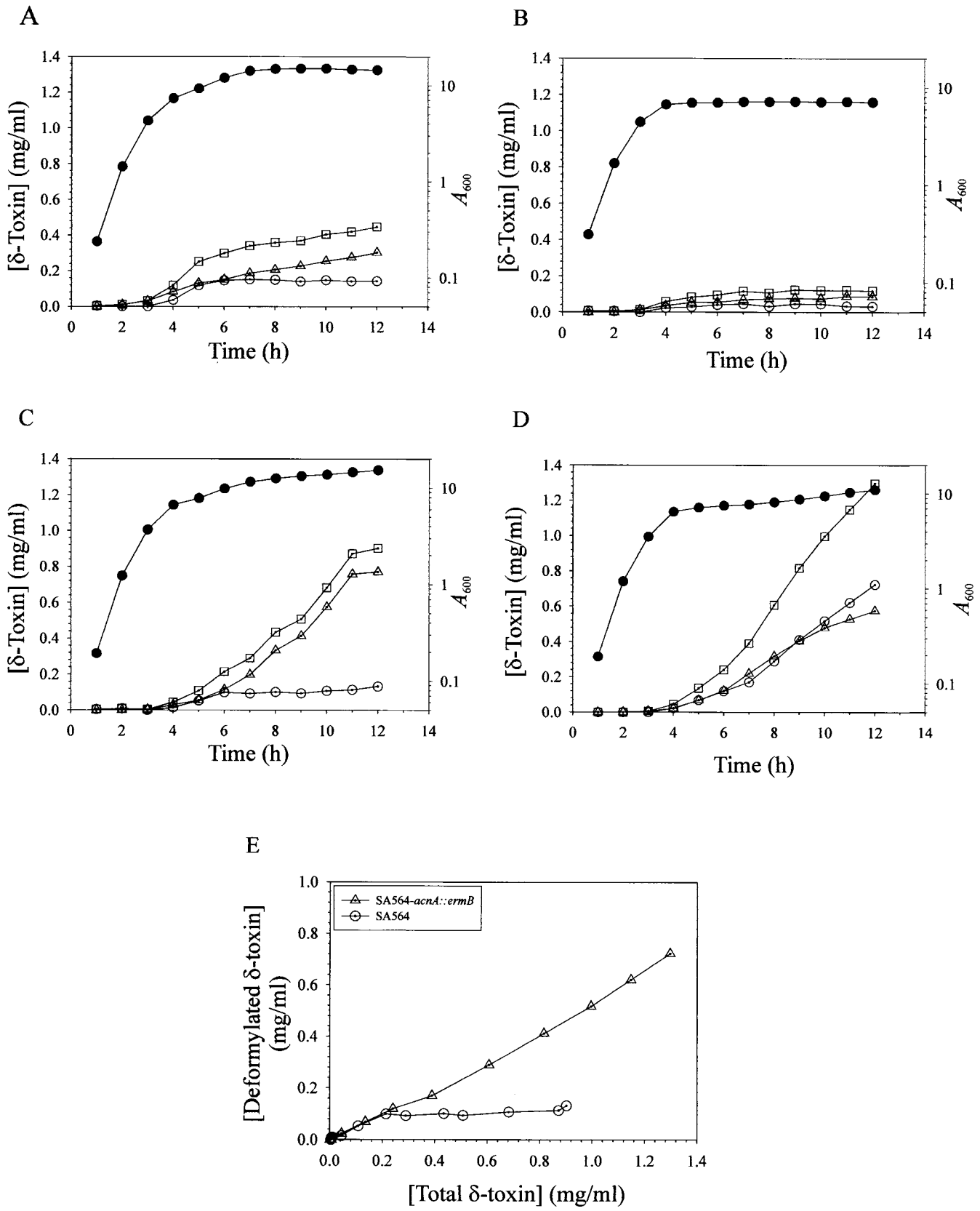


FIG. 1. Growth phase-dependent production of formylated δ-toxin and deformylated δ-toxin. Culture supernatants were harvested at hourly intervals, and δ-toxin concentrations were determined by HPLC. (A) Growth and δ-toxin production of strain SA564 grown in TSB. (B) Growth and δ-toxin production of strain SA564-*acnA*::*ermB* grown in TSB. (C) Growth and δ-toxin production of strain SA564 grown in TSB supplemented with 50 mM glutamate. (D) Growth and δ-toxin production of strain SA564-*acnA*::*ermB* grown in TSB supplemented with 50 mM glutamate. Symbols: ●, growth ($A_{600}$); □, total δ-toxin concentration; △, formylated δ-toxin concentration; ○, deformylated δ-toxin concentration. (E) Plot of the δ-toxin concentration data from panels C and D, showing the increased concentration of deformylated δ-toxin in the culture supernatant of the *acnA* mutant strain. The results are representative of the results of at least two independent experiments.

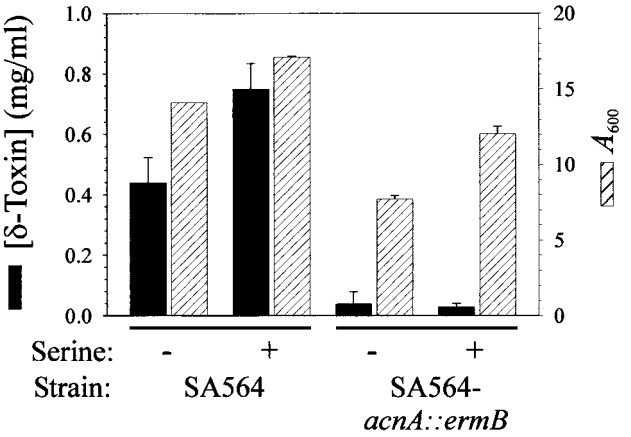


FIG. 2. Effect of supplemental serine on the growth yield and δ-toxin production of SA564 and SA564-*acnA*::*ermB*. Bacteria were grown for 12 h in TSB supplemented with 25 mM serine, and the growth yields ($A_{600}$) and δ-toxin concentrations were determined. The data are the means and standard errors of the means of two independent experiments.

δ-toxin production could be the result of insufficient glutamate. Supplementation of the culture medium with glutamate increased the growth yield and the total concentration of δ-toxin in both the wild-type and *acnA* mutant strains (Fig. 1C and D). These results suggest that the decreased production of δ-toxin by SA564-*acnA*::*ermB* compared to the production by parental strain SA564 was due to an inability to synthesize glutamate. δ-Toxin contains one glutamine but no glutamate residues; thus, glutamate auxotrophy likely indirectly affects δ-toxin synthesis. Of note, the total concentration of δ-toxin was greater in the culture supernatant from the wild-type strain grown with additional glutamate, but the concentration of deformylated δ-toxin was not altered compared to the concentration in a culture grown without additional glutamate (Fig. 1A and C). Thus, the entire increase in δ-toxin accumulation that occurred late in the postexponential and stationary phases of growth was attributable to the formylated form. Interestingly, aconitase inactivation dramatically increased the postexponential- and stationary-growth-phase deformylation of δ-toxin (Fig. 1D and E). These data suggest that the supply of another factor necessary for δ-toxin deformylation was limited and that the limiting factor was linked to TCA cycle activity.

*S. aureus* secretes several proteolytic enzymes into the culture medium during in vitro growth (6). Therefore, the decreased concentration of δ-toxin in the *acnA* mutant culture supernatant could have been caused by increased proteolytic activity. Analysis of the culture supernatants of SA564 and SA564-*acnA*::*ermB* demonstrated that the *acnA* mutant strain had total protease activity that was slightly lower than or the same as the total protease activity of the wild-type strain (data not shown). These results indicate that an increase in proteolytic activity in the culture supernatant was not the cause of the decreased δ-toxin concentration in the culture supernatant of the *acnA* mutant strain. Additionally, there are no known proteases produced by *S. aureus* that degrade δ-toxin.

TCA inactivation prevents the postexponential-growth-phase catabolism of acetate, resulting in a culture medium pH that is lower than the pH of the culture medium of the isogenic wild-type strain (24). Therefore, the lower pH of the culture medium of the *acnA* mutant strain may result in decreased production of δ-toxin. Supplementation of the culture medium with either serine or glutamate (Fig. 1 and 2) increased the production of $NH_3$ and raised the pH of the culture medium (Somerville, unpublished results). However, only supplemental glutamate increased the production of δ-toxin by the *acnA* mutant strain, demonstrating that the decreased production of δ-toxin by the *acnA* mutant strain compared to the production by the wild type was independent of pH.

**RNAIII transcription.** The concentration of δ-toxin in the culture medium of the *acnA* mutant strain could be increased by adding glutamate to the medium, suggesting that supplemental glutamate either enhanced translation of the existing message or increased the level of message available for translation or both. To examine these possibilities, strains SA564 and SA564-*acnA*::*ermB* were grown in TSB containing 50 mM glutamate, and a Northern blot analysis was performed with total RNA isolated at 2-h intervals throughout the growth cycle (Fig. 3). In agreement with previous results (24), the stationary-phase level of RNAIII was lower in the wild-type strain than in the *acnA* mutant (Fig. 3). Addition of supplemental

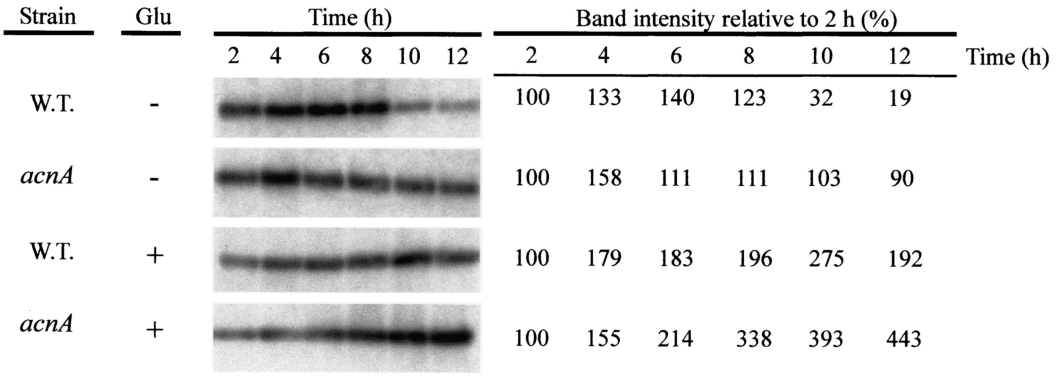


FIG. 3. Northern blot analysis of RNAIII expression. Total RNA was isolated from bacteria harvested at different times. Twenty micrograms of total RNA was used in each lane. To ensure that equivalent quantities of RNA were loaded, the RNA was visualized by ethidium bromide staining prior to transfer to a charged nylon membrane (data not shown). A radiolabeled probe specific for RNAIII was used. The band intensities relative to the band intensities for the 2-h time point are shown on the right. W.T., wild type.

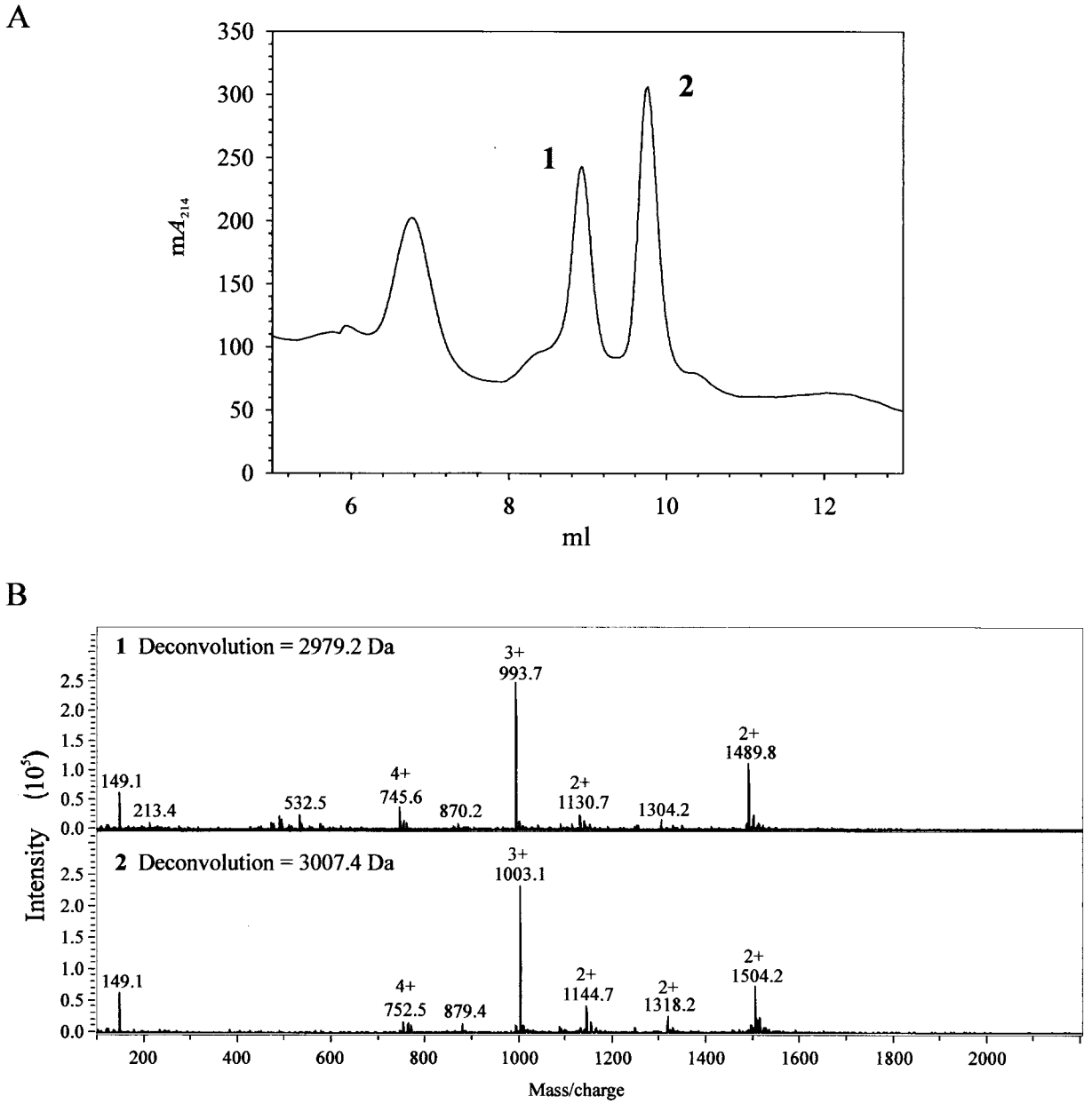


FIG. 4. Mass spectroscopic analysis of HPLC fractions containing formylated δ-toxin and deformylated δ-toxin. (A) Absorbance at 214 nm of SA564 culture supernatant fractionated by HPLC. Fractions containing peaks 1 and 2 were used for the mass spectroscopy analysis shown in panel B. (B) Mass spectrograms of peptides from fractions containing peaks 1 and 2 in panel A. The molecular masses of the peptides were 2,979.2 and 3,007.4 Da, corresponding to the deformylated and formylated δ-toxin peptides. The molecular mass of the formyl group is 28 Da.

glutamate to the culture medium extended the postexponential growth phases of both the wild-type and *acnA* mutant strains compared to the postexponential growth phases of similar bacterial cultures without glutamate (Fig. 1C and D), resulting in increased growth yields. Consistent with the extended postexponential growth phase of the wild-type strain, the level of RNAIII was also greater during the postexponential growth phase (Fig. 3). The level of RNAIII present in the *acnA* mutant strain increased dramatically during the postexponential growth phase and exceeded the level present in the *acnA* mutant grown in unsupplemented medium (Fig. 3). These data suggest that glutamate increased the level of *hld* (RNAIII) available for translation in the *acnA* mutant strain.

**δ-Toxin deformylation.** In bacteria, translation initiates with formyl-methionine. Usually, the amino-terminal formyl group is removed posttranslationally by the cytoplasmic peptide deformylase (encoded by *pdf1* in *S. aureus*). Interestingly, the predominant form of δ-toxin that accumulates in the culture medium contains a formylated N-terminal methionine residue (7, 25). HPLC analysis of culture supernatants from the wild-type and *acnA* mutant strains revealed the presence of two species of δ-toxin (Fig. 4). Mass spectroscopic analysis con-

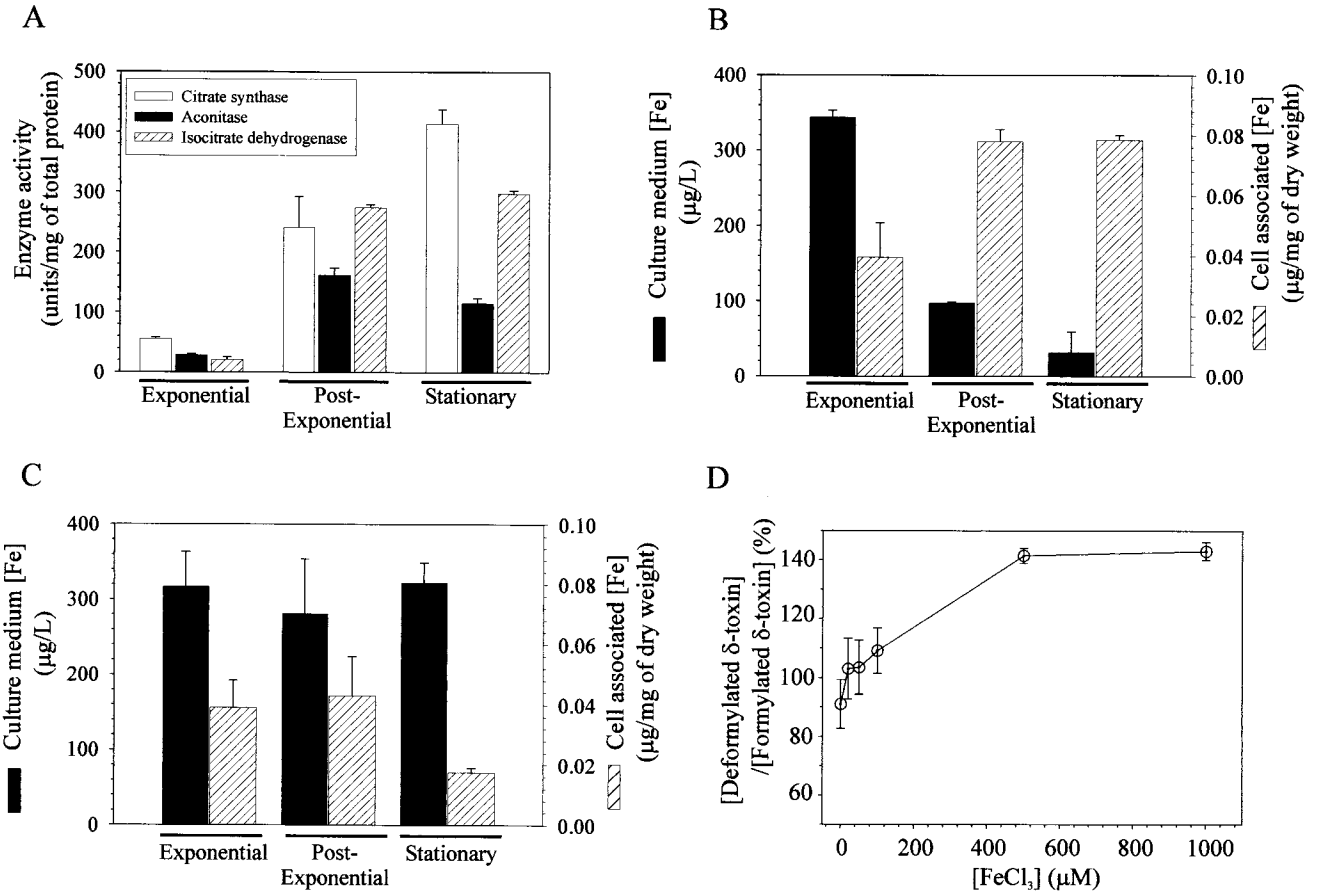


FIG. 5. *S. aureus* growth phase-dependent TCA cycle activity and iron depletion. (A) Citrate synthase, aconitase, and isocitrate dehydrogenase activities were determined in triplicate for two independent cultures during the exponential (3 h), postexponential (6 h), and stationary (12 h) phases of growth. (B and C) Iron concentrations in SA564 (B) and SA564-*acnA*::*ermB* (C) culture media and cell-associated iron concentrations during the exponential, postexponential, and stationary phases of growth. The concentration of iron in the culture medium prior to inoculation was 372 ± 44 μg/liter. (D) Effect of supplemental $FeCl_3$ on the ratio of deformylated δ-toxin to formylated δ-toxin. The data are means and standard errors of the means of at least two independent experiments.

firmed that the two δ-toxin species corresponded to the formylated and deformylated δ-toxin polypeptides (Fig. 4). During the exponential phase and part of the postexponential phase of growth, approximately 50% of the δ-toxin produced by wild-type strain SA564 was deformylated. In contrast, the concentration of deformylated δ-toxin was unchanged throughout the remainder of the growth cycle (Fig. 1A and C). These data demonstrate that δ-toxin deformylation is repressed or inhibited during the first 2 h of the postexponential growth phase and suggest that the decrease in deformylation may be the result of decreased expression of *pdf1*. Northern blot analysis of *pdf1* mRNA levels in the wild-type and mutant strains revealed equivalent *pdf1* transcript levels (data not shown), indicating that the postexponential-growth-phase inhibition of δ-toxin deformylation in the wild-type strain occurs independent of changes in the level of *pdf1* transcription.

Maximal TCA cycle activity occurs between the postexponential and stationary phases of growth (Fig. 5) and occurs contemporaneously with the reduction in δ-toxin deformylation (Fig. 1A). These data led us to speculate that there is a correlation between δ-toxin deformylation and TCA cycle activity. If there is a correlation, then the concentration of deformylated δ-toxin should be greater in the aconitase mutant strain than in the isogenic wild-type strain. As expected, the concentration of deformylated δ-toxin was significantly greater in the *acnA* mutant strain than in the wild-type strain (Fig. 1D and C). This was more evident when the concentrations of deformylated δ-toxin were plotted as a function of the total δ-toxin concentrations (Fig. 1E). These results and the equivalent *pdf1* transcript levels suggest that induction of TCA cycle activity inhibits the deformylation of δ-toxin.

**Iron limitation.** The *S. aureus* TCA cycle includes at least two iron-requiring enzymes or enzyme complexes: aconitase and succinate dehydrogenase. (The *S. aureus* fumarase is a *fumC* homologue and as such probably does not require iron.) The postexponential-growth-phase induction of TCA cycle activity creates a demand for iron in wild-type *S. aureus*. The increased demand for iron coincides with the loss of δ-toxin deformylation (Fig. 1A and 5). As noted above, peptide deformylase removes the amino-terminal formyl group of formylmethionine, an enzymatic activity that requires iron (2), which led us to hypothesize that the loss of δ-toxin deformylation was the result of iron limitation. We measured the concentrations of iron in the culture media and cell pellets of the wild-type

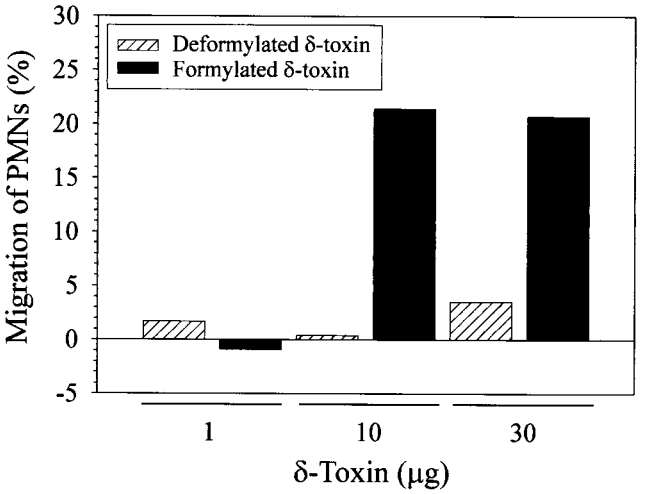


FIG. 6. δ-Toxin-induced polymorphonuclear leukocyte (PMN) migration. The percentage of neutrophils migrating toward δ-toxin was calculated as described in Materials and Methods. The results are representative of three independent experiments in which three separate polymorphonuclear leukocyte donors were used.

and *acnA* mutant strains during the exponential, postexponential, and stationary phases of growth (Fig. 5B and C). As expected, the wild-type strain depleted the culture medium of iron between the postexponential and stationary phases of growth; however, the majority of iron remained in the culture medium of the *acnA* mutant strain throughout the growth cycle. Correspondingly, the amount of cell-associated iron increased significantly in the wild-type strain during the transition from the exponential growth phase to the postexponential growth phase, but this did not occur in the *acnA* mutant strain. Thus, supplementation of the culture medium with iron should increase the concentration of deformylated δ-toxin and decrease the concentration of formylated δ-toxin in the culture medium of the wild-type strain. To test this possibility, strain SA564 was grown for 12 h in culture medium supplemented with $FeCl_3$, and the ratio of the concentration of deformylated δ-toxin to the concentration of formylated δ-toxin was determined (Fig. 5D). The ratio of the concentration of deformylated δ-toxin to the concentration of formylated δ-toxin for strain SA564 grown in TSB increased as the concentration of supplemental iron increased. These data strongly suggest that induction of the TCA cycle during the postexponential growth phase results in an increased demand for iron. Additionally, these data indicate that if insufficient iron is available (as would be encountered during an infection in which free iron is present in human blood at a concentration of $10^{-18}$ M) to support TCA cycle activity, then iron is diverted from iron-containing enzymes (e.g., peptide deformylase) to facilitate TCA cycle activity.

**Neutrophil chemotaxis.** Peptides with an N-terminal formylmethionine are potent neutrophil chemoattractants, whereas the equivalent deformylated peptides are not (21). Hence, we speculated that formylated δ-toxin would attract human neutrophils but that the deformylated δ-toxin would not attract neutrophils. Consistent with our hypothesis, we found neutrophil chemotaxis activity only with formylated δ-toxin (Fig. 6). For example, 16.0% ± 5.0% of neutrophils migrated toward 10 μg of formylated δ-toxin, whereas 2.2% ± 2.7% of neutrophils migrated toward 10 μg of deformylated δ-toxin ($P = 0.003$). These data demonstrate that δ-toxin deformylation has functional consequences.

## DISCUSSION

**Current model of δ-toxin synthesis.** The synthesis of many *S. aureus* virulence factors is regulated through an unknown mechanism by RNAIII, which is part of the *agr* locus (17). Structural mapping and computer modeling have led to the prediction that RNAIII is a highly ordered molecule containing 14 hairpin structures connected by unpaired nucleotides (3). In addition to its regulatory function, RNAIII is the message for δ-toxin (*hld*) (11). Translation of *hld* occurs approximately 1 h after transcription of RNAIII; however, the delay can be alleviated by deletion of the 3′ end of RNAIII (1). These observations suggest that RNAIII must undergo a conformational change before translation can occur (1, 3). In this model of δ-toxin translation, there is no prerequisite for factors other than ribosomes and RNAIII; however, the model does not preclude the possibility that other factors may be required for translation.

**Aconitase and δ-toxin synthesis.** Inactivation of *S. aureus acnA* resulted in a significantly elevated stationary-phase level of RNAIII compared to the level in the wild-type strain (24). Based on the current understanding of δ-toxin production, these data led us to hypothesize that aconitase inactivation should increase the production of δ-toxin. However, *acnA* inactivation drastically decreased the total stationary-phase concentration of δ-toxin (Fig. 1A and B). The concentration of δ-toxin was increased more than 10-fold by supplementing the culture medium with glutamate (Fig. 1B and D), suggesting that the decreased δ-toxin production was the result of glutamate auxotrophy. However, addition of glutamate also increased the level of RNAIII in the *acnA* mutant strain (Fig. 3). Taken together, these data indicate that aconitase inactivation increases the production or stability of RNAIII but that glutamate auxotrophy prevents translation of *hld*. This also raises an important question: Why does aconitase inactivation increase the production or stability of RNAIII? A possible explanation for the increased production and/or stability of RNAIII in the aconitase mutant strain may lie in the fact that aconitase exhibits 52% amino acid identity to the eukaryotic cytosolic aconitase known as iron-responsive protein 1 (IRP-1). IRP-1 is an RNA-binding protein that recognizes a specific RNA hairpin structure called the iron-responsive element (IRE). IREs were first identified in the 5′ untranslated regions (UTRs) of the ferritin H-chain and in the 3′ UTR of the tranferrin receptor mRNA (5, 10). Binding of IRP-1 to an IRE present in the 5′ UTR of an mRNA blocks translation by preventing association of the ribosomal complex with the mRNA (9). When the IRE(s) is present in the 3′ UTR of the mRNA, binding of IRP-1 stabilizes the message, which allows increased translation (5). RNAIII is a highly ordered molecule, which raises the possibility that aconitase may bind to a hairpin structure of RNAIII and affect its stability. The role of aconitase in the stability or production of RNAIII is under investigation.

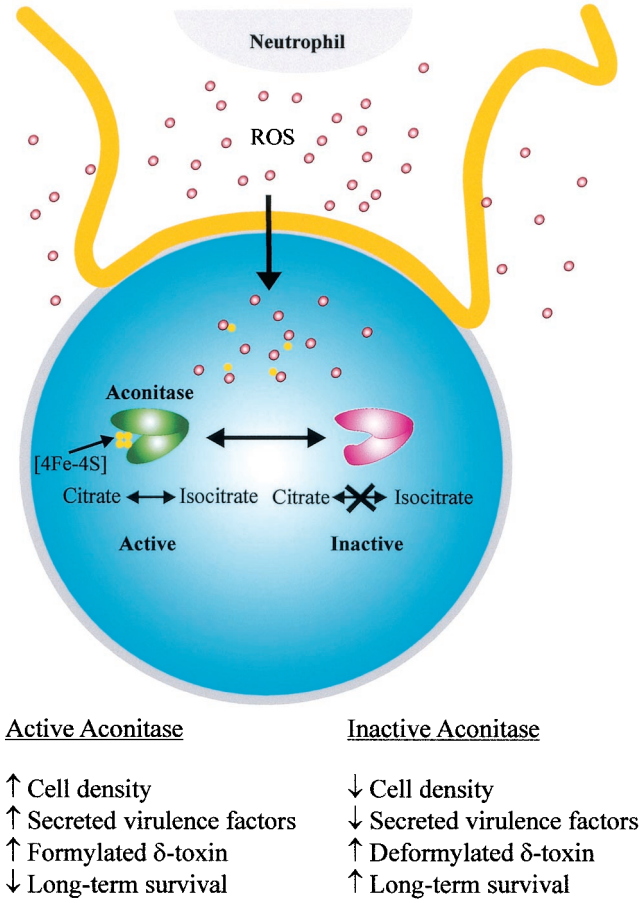


FIG. 7. Model for reactive oxygen species (ROS)-mediated aconitase inactivation and the consequences of such inactivation. Neutrophils initiate an oxidative burst upon contact with bacteria and as a result produce ROS. ROS, in addition to being targeted toward phagocytic vesicles (data not shown), nonspecifically permeate the neutrophil membrane, which allows some ROS to penetrate the bacterial membrane (shown being engulfed by a neutrophil). Once inside the bacterial cell, the ROS oxidize the fourth iron atom of the [4Fe-4S] cluster, resulting in formation of a [3Fe-4S] iron-sulfur center (a similar reversible inactivation can occur during growth under iron- or substrate-limiting conditions). This oxidation is sufficient to reversibly inactivate aconitase. The [3Fe-4S] cluster can undergo further reversible disassembly to generate the iron-free apo-aconitase. Once ROS production has ceased or bacterial antioxidant defenses limit the effects of ROS toxicity, the iron-sulfur cluster of aconitase can be reassembled, which allows enzymatic conversion of citrate to isocitrate.

**δ-Toxin deformylation.** δ-Toxin has been reported to accumulate in *S. aureus* culture medium in both the formylated (approximately 90%) and deformylated (approximately 10%) forms (7, 23). The accumulation of deformylated δ-toxin in the culture medium unexpectedly stops during the postexponential growth phase (Fig. 1A and C). In contrast, formylated δ-toxin continues to accumulate, thus accounting for the large disparity in the concentrations of formylated δ-toxin and deformylated δ-toxin. The transition from producing both species of δ-toxin to producing only the formylated δ-toxin occurred concomitant with maximal TCA cycle induction and depletion of iron from the culture medium (Fig. 5). This repression of δ-toxin deformylation could be relieved by TCA cycle inactivation or addition of supplemental iron to the culture medium (Fig. 1E and 5D), suggesting that δ-toxin deformylation is linked to iron availability.

**Implications for aconitase inactivation in vivo.** Aconitase is a TCA cycle enzyme that converts citrate to isocitrate via a *cis*-aconitate intermediate. The enzymatic function is mediated by an [4Fe-4S] iron-sulfur center that is necessary for binding of the substrate. Three of the iron atoms in the [4Fe-4S] center are coordinately bound by three conserved cysteine residues. The fourth iron atom is held in place by a molecule of substrate and water (12). In the absence of substrate, the fourth iron atom is susceptible to reversible inactivation by oxygen radicals (8). As part of the innate immune response, phagocytic leukocytes produce reactive oxygen species to limit the growth and dissemination of bacteria. Hence, it is reasonable to hypothesize that early in an infection aconitase is reversibly inactivated, resulting in decreased production of formylated δ-toxin (Fig. 1B), a chemoattractant for human leukocytes (Fig. 6). Taken together, these data led us to speculate that reversible inactivation of aconitase suppresses the proinflammatory immune response (Fig. 7). It has been reported previously that aconitase inactivation significantly decreases virulence factor production and enhances stationary-phase survival (24). Thus, reversible oxidative inactivation of aconitase should reduce inflammation, decrease the production of virulence factors, and promote bacterial survival.

## ACKNOWLEDGMENTS

We thank T. A. Tran, R. Young, and J. Trias for helpful suggestions, H. Caldwell for a critical review of the manuscript, and G. Hettrick for help with figure preparation.

## REFERENCES

1. **Balaban, N., and R. P. Novick.** 1995. Translation of RNAIII, the *Staphylococcus aureus agr* regulatory RNA molecule, can be activated by a 3′-end deletion. FEMS Microbiol. Lett. **133:**155–161.
2. **Baldwin, E. T., M. S. Harris, A. W. Yem, C. L. Wolfe, A. F. Vosters, K. A. Curry, R. W. Murray, J. H. Bock, V. P. Marshall, J. I. Cialdella, M. H. Merchant, G. Choi, and M. R. Deibel, Jr.** 2002. Crystal structure of type II peptide deformylase from *Staphylococcus aureus*. J. Biol. Chem. **277:**31163–31171.
3. **Benito, Y., F. A. Kolb, P. Romby, G. Lina, J. Etienne, and F. Vandenesch.** 2000. Probing the structure of RNAIII, the *Staphylococcus aureus agr* regulatory RNA, and identification of the RNA domain involved in repression of protein A expression. RNA **6:**668–679.
4. **Bhakoo, M., T. H. Birkbeck, and J. H. Freer.** 1982. Interaction of *Staphylococcus aureus* delta-lysin with phospholipid monolayers. Biochemistry **21:**6879–6883.
5. **Casey, J. L., M. W. Hentze, D. M. Koeller, S. W. Caughman, T. A. Rouault, R. D. Klausner, and J. B. Harford.** 1988. Iron-responsive elements: regulatory RNA sequences that control mRNA levels and translation. Science **240:**924–928.
6. **Dubin, G.** 2002. Extracellular proteases of *Staphylococcus* spp. Biol. Chem. **383:**1075–1086.
7. **Fitton, J. E., A. Dell, and W. V. Shaw.** 1980. The amino acid sequence of the delta haemolysin of *Staphylococcus aureus*. FEBS Lett. **115:**209–212.
8. **Gardner, P. R., and I. Fridovich.** 1992. Inactivation-reactivation of aconitase in *Escherichia coli.* A sensitive measure of superoxide radical. J. Biol. Chem. **267:**8757–8763.
9. **Gray, N. K., and M. W. Hentze.** 1994. Iron regulatory protein prevents binding of the 43S translation pre-initiation complex to ferritin and eALAS mRNAs. EMBO J. **13:**3882–3891.
10. **Hentze, M. W., S. W. Caughman, T. A. Rouault, J. G. Barriocanal, A. Dancis, J. B. Harford, and R. D. Klausner.** 1987. Identification of the iron-responsive element for the translational regulation of human ferritin mRNA. Science **238:**1570–1573.
11. **Janzon, L., S. Lofdahl, and S. Arvidson.** 1989. Identification and nucleotide sequence of the delta-lysin gene, *hld*, adjacent to the accessory gene regulator (*agr*) of *Staphylococcus aureus*. Mol. Gen. Genet. **219:**480–485.
12. **Kennedy, M. C., M. Werst, J. Telser, M. H. Emptage, H. Beinert, and B. M.**

**Hoffman.** 1987. Mode of substrate carboxyl binding to the $[4Fe\text{-}4S]^{+}$ cluster of reduced aconitase as studied by $^{17}O$ and $^{13}C$ electron-nuclear double resonance spectroscopy. Proc. Natl. Acad. Sci. USA **84:**8854–8858.

13. **Lazennec, C., and T. Meinnel.** 1997. Formate dehydrogenase-coupled spectrophotometric assay of peptide deformylase. Anal. Biochem. **244:**180–182.
14. **Lowry, O. H., N. J. Rosebrough, L. Farr, and R. J. Randall.** 1951. Protein measurement with the Folin phenol reagent. J. Biol. Chem. **193:**267–275.
15. **Morfeldt, E., L. Janzon, S. Arvidson, and S. Lofdahl.** 1988. Cloning of a chromosomal locus (*exp*) which regulates the expression of several exoprotein genes in *Staphylococcus aureus*. Mol. Gen. Genet. **211:**435–440.
16. **Novick, R. P.** 2000. Pathogenicity factors and their regulation, p. 392–407. *In* V. A. Fischetti, R. P. Novick, J. J. Ferretti, D. A. Portnoy, and J. I. Rood (ed.), Gram-positive pathogens. ASM Press, Washington D.C.
17. **Novick, R. P., H. F. Ross, S. J. Projan, J. Kornblum, B. Kreiswirth, and S. Moghazeh.** 1993. Synthesis of staphylococcal virulence factors is controlled by a regulatory RNA molecule. EMBO J. **12:**3967–3975.
18. **Otto, M., and F. Gotz.** 2000. Analysis of quorum sensing activity in staphylococci by RP-HPLC of staphylococcal delta-toxin. BioTechniques **28:**1088, 1090, 1092, 1096.
19. **Peng, H. L., R. P. Novick, B. Kreiswirth, J. Kornblum, and P. Schlievert.** 1988. Cloning, characterization, and sequencing of an accessory gene regulator (*agr*) in *Staphylococcus aureus*. J. Bacteriol. **170:**4365–4372.
20. **Sambrook, J., E. F. Fritsch, and T. Maniatis.** 1989. Molecular cloning: a laboratory manual, 2nd ed. Cold Spring Harbor Laboratory Press, Plainview, N.Y.
21. **Schiffmann, E., B. A. Corcoran, and S. M. Wahl.** 1975. N-formylmethionyl peptides as chemoattractants for leucocytes. Proc. Natl. Acad. Sci. USA **72:**1059–1062.
22. **Schmitz, F. J., K. E. Veldkamp, K. P. Van Kessel, J. Verhoef, and J. A. Van Strijp.** 1997. Delta-toxin from *Staphylococcus aureus* as a costimulator of human neutrophil oxidative burst. J. Infect. Dis. **176:**1531–1537.
23. **Smith, G. M., and W. V. Shaw.** 1981. Comparison of three methods for the purification of the delta haemolysin of *Staphylococcus aureus*. J. Gen. Microbiol. **124:**365–374.
24. **Somerville, G. A., M. S. Chaussee, C. I. Morgan, J. R. Fitzgerald, D. W. Dorward, L. J. Reitzer, and J. M. Musser.** 2002. *Staphylococcus aureus* aconitase inactivation unexpectedly inhibits post-exponential-phase growth and enhances stationary-phase survival. Infect. Immun. **70:**6373–6382.
25. **Thomas, D. H., D. W. Rice, and J. E. Fitton.** 1986. Crystallization of the delta toxin of *Staphylococcus aureus*. J. Mol. Biol. **192:**675–676.
26. **Troelstra, A., B. N. Giepmans, K. P. Van Kessel, H. S. Lichenstein, J. Verhoef, and J. A. Van Strijp.** 1997. Dual effects of soluble CD14 on LPS priming of neutrophils. J. Leukoc. Biol. **61:**173–178.
27. **Veldkamp, K. E., H. C. Heezius, J. Verhoef, J. A. van Strijp, and K. P. van Kessel.** 2000. Modulation of neutrophil chemokine receptors by *Staphylococcus aureus* supernate. Infect. Immun. **68:**5908–5913.
28. **Vuong, C., H. L. Saenz, F. Gotz, and M. Otto.** 2000. Impact of the *agr* quorum-sensing system on adherence to polystyrene in *Staphylococcus aureus*. J. Infect. Dis. **182:**1688–1693.
29. **Weitzman, P. D. J.** 1969. Citrate synthase from *Escherichia coli*. Methods Enzymol. **13:**22–26.
30. **Williamson, J. R., and B. E. Corkey.** 1969. Assays of intermediates of the citric acid cycle and related compounds by fluorometric enzyme methods. Methods Enzymol. **13:**434–513.